MODELLING OF DEPOSITION PHENOMENA IN LOW ENTHALPY GEOTHERMAL WELLS

Afif Abou Akar and Ioannis Ignatiadis

BRGM, Research Division, Department of Geotechnical Engineering and Mineral Technology,
Avenue de Concyr, BP 6009,45060 Orléans, (France)

Key words: geothermal well. corrosion, deposition, iron sulphide, modelling scaling, diffusion layer.

Abstract

The well casings (most of which are of carbon steel) of geothermal plants exploiting the Dogger aquifer in the Paris Basin experience problems of corrosion and scaling related to the aggressivity of the geothermal fluid and to the precipitation of iron sulphides, mainly as mackinawite A chemical code, MODEP, using a predetermined uniform corrosion rate and allowing a simulation of mackinawite scaling on the casing wall is proposed. Calculations based on mass conservation and mass balance enable us to: (i) calculate the distribution of dissolved or degassed chemical species in the fluid as a function of temperature and pressure; (ii) calculate the saturation indexes of the fluid with respect to the various minerals; (iii) evaluate the excess of ferrous iron precipitated as mackinawite and (iv) calculate the new diameter of the casing. The basic data necessary for this model is the borehole fluid chemical composition. Two methods were used to sample the fluid: sampling with an inert bottom sampler and at the wellhead with a special composite tubing. Dissolved iron and total sulphide, measured in the production wellhead and calculated by MODEP are in a good agreement. This work continues in order to study diffusion phenomena and concentration gradients near the well wall and to improve knowledge of iron sulphide precipitation kinetics.

1. INTRODUCTION - OBJEC'I'IVE

There are several reasons why mathematical models are needed in the field of geothermal energy Laboratory and in situ experiments are costly, and computer tools can tahe a number of reactions into account simultaneously and simulate the effects of variations in the parameters of the geothermal fluid The behaviour of a fluid at various temperatures and pressures can be simulated with existing geochemical computer codes These simulations take into account the gaseous phase, but do not, or only partly take into consideration precipitation phenomena which may accompany these variations The modelling of corrosion and scaling phenomena is very useful since these phenomena are the main problem encountered in geothermal plants Carbon steel casing can be perforated by localised corrosion, and scaling increases the head loss in the well and reduces the flow rate Modelling of these phenomena allows the geothermal plant operator to predict corrosion and scaling evolution and choose optimal exploitation parameters

2. PRELIMINARY CONSIDERATIONS, BLBLIOGRAPHIC STUDY AND STATE OF PROGRESS

2.1. Preliminary considerations

Before attempting to model the phenomena of corrosion and scaling, it must be understood that it is difficult to develop an ideal model Several factors must be taken into consideration

(i) There are various types of corrosion of carbon steel uniform, crevice and pitting

(ii) Knowledge of the diffusion layer (the thickness of which depends on the Reynolds number) is very important, for it is in this layer, next to the well wall, that the main precipitation reactions take place Species concentrations vary within this layer along concentration gradients so they can therefore be expressed versus their distance from the metal as $Fe^{2+}(x)$ $H^+(x)$ and **A-(x)** (fig 1), allowing the calculation of a solubility product $K_s(x)$ In the fluid vein (convexion layer), concentrations are uniform

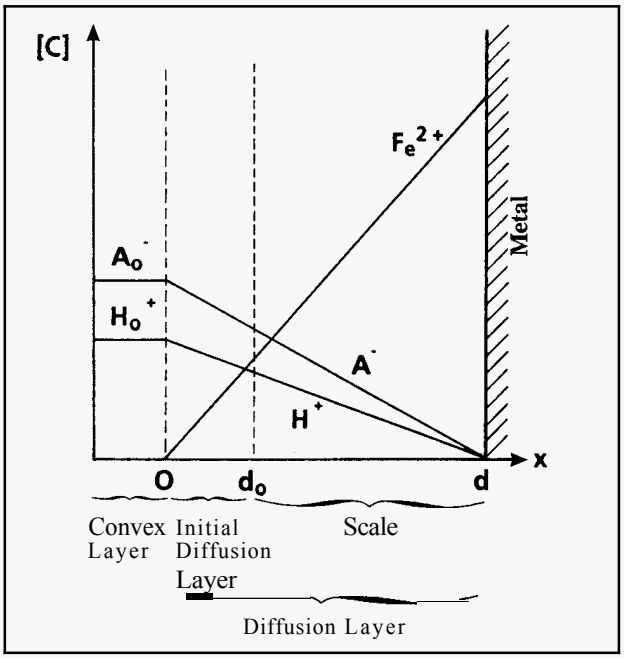

Figure 1: Concentration profiles of Fe^{2+}, $H^+$and **A-** in the diffusion layer.

(iii) A large number of competitive precipitation and dissolution reactions take place. Reaction kinetics must therefore be taken into account.

(iv) The model must be validated by comparing the calculated results, in both type and quantity, with data gathered on site by logs, coupon tests and microscopic examination of the scale.

2.2. Bibliographic study

As indicated by its E_h-pH diagram (Pourbaix and Pourbaix, 1981), iron does not coexist peacefully with water. The line of reduction of H^+ ions is located totally outside of the domain of metallic iron. When a piece of iron is placed in an aqueous solution, a redox couple is created spontaneously along the following scenario:

at the anode: $Fe \rightarrow Fe^{2+} + 2e^-$ (1)

at the cathode: $2H^+ + 2e^- \rightarrow H_2$ (2)

which will maintain the corrosion of the iron. This reaction, moderate in distilled water, will increase strongly in the presence of other species such as carbonates CO_2/HCO_3^-, sulphides H_2S/HS^- and chloride Cl^-. These species, and according to the saturation indexes of their mineral with iron, can precipitate the iron produced by corrosion and favour the corrosion reaction by facilitating the removal of Fe^{2+}. The dissolved weak acids (H_2CO_3, H_2S) also maintain the corrosion by facilitating the transport of H^+ ions in the non deprotonated form towards the cathode (De Waard and Milliams, 1975).

In solution, an iron gradient will be established in the immediate vicinity of the metal (limit layer). The iron produced will migrate by diffusion in this layer according to Fick's law towards the fluid vein, made up of all of the solution, where it is removed by convection.

$$J_{Fe} = - D_{Fe} \text{ grad } Fe \quad (3)$$

J_{Fe} is the iron flux and D_{Fe} is the diffusion coefficient of iron.
For a monodirectional migration:

$$J_{Fe} = - D_{Fe} \partial Fe/\partial x \quad (3')$$

This leads, after a second derivative of Fe(x) to:

$$\partial Fe_{tot}/\partial t = - V J_{Fe} = D.\partial^2 Fe_{tot}/\partial x^2 = 0 \text{ in the steady state} \quad (4)$$

(V is the $\partial^2/\partial x^2$ operator).

This iron gradient is balanced by a gradient of the other species (such as H^+) so that in all points in the diffusion layer, the electrical neutrality of the solution is respected.

$$2\,Fe^{2+} + H+ + \Sigma\, n_i\,.\,C_i = \Sigma\, n_i\,.\,A_i \quad (5)$$

n_i : charge of the species i

The sulphide ions are consumed at the surface of the metal by the precipitation reaction of the iron sulphides. The sulphide (or anion, in the general case) content near the metal controls the regulation of the iron sulphide (salt) deposit. In this way, a depletion in anions leads to an anionic insoluble deposit (non protective, control of scale by the anion which is depleted near the metal). while an abundance of anion makes the iron control the process of the scale formation leading either to a soluble deposit or a cationic insoluble deposit (the latter is protective) (Crolet. 1988, 1990).

To the term relative to the chemical diffusion used in the Fick equation we must add other terms which enable us to express the mass conservation law for each chemical species at every point in the diffusion layer. In addition to chemical diffusion, this generalised equation takes into account:

- the reactional term: species produced and species consumed by reactions taking place in the diffusion layer,
- the electromigration term or diffusion under an electric field as opposed to that of simple chemical diffusion. The origin of this is the existence of an electromigration potential (V) also called the diffusion potential (Crolet, 1988; Sharland and Tasker, 1988; Sharland 1988; Watson and Postlethwaite, 1990). This electromigration potential groups two terms:
  - one is its first derivative grad $V = \partial V/\partial x$,
  - the other is its second derivative $\nabla V = \partial^2 V/\partial x^2$.

The expression of the first term "grad V" as a function of the ionic strengh "I" of the solution reveals that it is proportional to the term "[Fe]/2.I" (Crolet, 1988). We can thus distinguish the media which are "more salty than acidic" with chemical diffusion of the ion and the media "more acidic than salty" with electromigration of the ion. The "grad V" term becomes negligible in the case of a solution of average salinity (such as water in the Dogger aquifer) which enables us to eliminate it from the mass conservation equation. The second term "∇V" is governed by the Poisson equation:

$$\nabla V = - \sigma/\varepsilon \quad (6)$$

$$\text{with } \sigma = F\,.\,\Sigma\, n_i\ J_i \quad (7)$$

where

- σ current density
- ε permittivity of the electrolyte
- F Faraday number
- n_i charge of the species i
- J_i flux of the species i

This equation is often replaced by the equation of electroneutrality in the solution

$$\Sigma\, n_i\ C_i = 0, \quad (C_i \text{ species i concentration}) \quad (5')$$

The reactional term was introduced by Sharland and Tasker (1988), Sharland (1988) and Walton (1988) in their mathematical model in the form of a reaction rate Equations including rate constants were added to the transport equation These terms in the case of a reaction

$$A + B \underset{k_{-1}}{\overset{k_1}{\Leftrightarrow}} C + D \underset{k_{-2}}{\overset{k_2}{\Leftrightarrow}} E + F \quad (8)$$

are expressed in the following way:

- For a species which reacts like A or B

$$- k_1 [A] [B] + k_{-1} [C] [D] \quad (9)$$

- For a species which is produced like E or F

$$k_2 [C] [D] - k_{-2} [E] [F] \quad (10)$$

- For a intermediate species like C or D

$$k_1 [A] [B] - k_{-1} [C] [D] + k_2 [C] [D] - k_{-2} [E] [F] \quad (11)$$

The rate constants bring usually unknown, the system can be solved by a rearrangement of equations in such a way as to eliminate the k_i terms (Sharland, 1988. Walton, 1988)

Grande and Talbot (1993) preferred treating the problem in a different way to simulate electrodeposition of coatings of iron-nickel at the cathode They used the mass action law to express the concentration of iron or nickel complexes as a function ot the simple chemical species and equilibrium constants of the concerned reactions rhese concentrations were then derived with respect to the element dx (advancement in the diffusion layer) This method *ot* derivation is systematically used in geochemical computer codes such as FQ3 6 (Wolery *et al* 1988) SOLMINEQ (Kharaka *et al.*, 1988) and TPDFGAZ (Czernikowski-Lauriol 1988) where the equilibrium constant is derived with respect to temperature or pressure

Nesic (1993) prefered to treat the problem in a simpler way. Fick's diffusion law was reduced to its simplified form (chemical diffusionj. For the flux of the species being studied (H^+, OH^-. $CO_2/H_2CO_3/HCO_3^-/CO_3^{2-}$, Fe^{2+}), he expressed equilibrium constants, but without involving the iron in the various equilibria existing in the solution and he added the equation of electrical neutrality. The author calculated the thickness of the diffusion layer and then set the limit conditions for each layer (concentrations of chemical species along the metal wall and in contact with the solution). Two species were chosen as references. After each increment (using the finite difference method). the concentrations in other species were recalculated so that at all points of the diffusion layer, the above equation remain verified

2.3. Calculation of the thickness of the diffusion layer

To calculate the thickness of the diffusion layer on the casing walls, we used the method proposed by Berger and Hau (1977) described below

$$\delta_c = d_h / Sh \quad (12)$$

$$\text{with } Sh = k\,.\,d_h / D_i = 0.0165\,.\,Re^{0.86}\ Sc^{0.33} \quad (13)$$

where:

- δ_c : thickness of the limiting diffusion layer (cm)
- d_h : hydraulic diameter of the casing (cm)
- D_i . diffusion coefficient of species i ($cm^2.s^{-1}$)
- Re : Reynolds number
- Sc : Schmidt number
- Sh : Sherwood number

The numerical application to a fluid for working conditions similar to those encountered in geothermal exploitations (among others, a turbulent regime) gives a diffusion layer thickness of around 12 µ Some specialists consider this value to be too high for exploitation in turbulent regimes.

2.4. Boundary conditions

As stated above, there are different concentrations of chemical species on either side of the diffusion layer. On the fluid vein side. that is to say for all of the geothermal fluid, the concentration of each species is taken as being equal to that of its concentration in the fluid. On the casing wall side, the concentrations of the carious species are harder to determine. The iron content is much higher because of the input by corrosion of the casing steel. An iron gradient is therefore established and the iron moves by diffusion to the fluid vein. This iron tlux is balanced by the opposite flux of H^+ ions as well as by a consumption of Fe^{2+} ions by the anions of the solution to form complexes (charged or neutral) and precipitates

Fe^{2+}, H^+, and HS- ion activities near the casing wall must satisfy the following condition

$$(Fe^{2+})\,.\,(HS^-)/(H^+) < \text{or} = K_s \quad (14)$$

where K_s is the solubility product of mackinawite. Indeed, we have shown (Peyrot, 1993; Ignatiadis and Peyrot, 1994) that mackinawite is the iron sulphide which controls the solubility of iron and sulphides in the geothermal fluids of the Dogger of the Paris basin.

The iron concentration on the casing walls can be calculated by integration of Ficks law. We have applied this law combining it with the formula already used in the MODEP computer code to calculate, at each increment, the iron supply into the medium following the corrosion of casings. Starting at the bottom of the well, and assuming that the iron concentration in the reservoir [Fe], is known [bottom hole sampling (Boisdet *et al.*, 1992) or that iron is in equilibrium with pyrite], we can write:

$$[Fe]_{wall} = \delta_o.J_o/D + [Fe]_o = \delta_o.K.V_o/D + [Fe], \quad (15)$$

D iron diffusion coefficient ($cm^2\ s^{-1}$)
V_o initial corrosion rate ($cm\ s^{-1}$)
δ_o thickness of the diffusion layer (cm)
K coefficient such as $J_o = f(V_o)$ grouping a series of parameters relative to the well and the geothermal fluid

In previous work (Boisdet *et al* , 1992. Abou Akar and Ignatiadis, 1994), we calculated at each ΔZ increment (Z being the depth of the well) and for all of the fluid vein (in the absence of a diffusion layer), an average concentration in dissolved iron due to the corrosion of casing For an iron diffusion coefficient (D_{Fe}) equal to 10^{-5} $cm2\ s^{-1}$ and a diffusion layer thickness of 12 µ, the dissolved iron content on the casing walls is 480 times higher than the average iron concentration calculated in the fluid vein Assuming that the iron removed by diffusion from the wall leads to this average iron concentration, we can calculate the new iron concentration at each increment

$$([Fe]_o)_1 = ([Fe]_o)_{reservoir} + \text{diffused iron (1st supply by corrosion)} \quad (16)$$
$$([Fe]_o)_i = ([Fe]_o)_{i-1} + \text{diffused iron (i}^{th}\text{ supply by corrosion)} \quad (16')$$

The iron on the casing wall will also be incremented at each ΔZ step

$$([Fe]_{wall})_1 = ([Fe]_o)_{reservoir} + \delta_o.K.V_o/D \quad (15')$$
$$([Fe]_{wall})_i = ([Fe]_{wall})_{i-1} + \delta_o.K.V_o/D \quad (15'')$$

2.5. State of progress

Application of the mass conservation law

The bibliographic study revealed that authors always reduce the number ofspecies to the minimum necessary in order to simplify the problem and be able to solve the system of non-linear equations by the finite element or difference method. Indeed, a large number of chemical elements (simple and compound species) would render the system very complex and the calculation too lengthy. Therefore, and in order to simplify the problem to be solved, the number of species which can be treated with our MODEP code will be small. The number of simple species has been reduced from 18 to 7, the complex species from 42 to 11 and the mineral species from 19 to 1. Free gasses have been set aside for the time being. The new system can be summarised as follows:

Simple species:
H, OH-, Fe^{2+}, Na^+, HS-, Cl-, CO_3^{2-}

Complex species (soluble):
H_2, H_2S, H_2CO_3, HCO_3^-, $FeHCO_3^+$, $FeCO_3$, $FeCl^+$, $Fe(HS)_3^-$, $Fe(HS)_2$, $NaHCO_3$, $NaCO_3^-$

Mineral species:
$Fe_{1+x}S_{(s)}$ (mackinawite)

Equilibria:
Complex and mineral species are supposed to be in equilibria with simple species; the concentrations in complex species can thus be expressed as a function of the concentrations in simple species. In the case of $FeHCO_3^+$ this will give.

$$\{FeHCO_3^+\} = K\gamma/K_{(T,P)}\{Fe^{2+}\}\{H^+\}\{CO_3^{2-}\} \quad (17)$$

$K_{(T,P)}$ equilibrium constant
$K\gamma$ activity coeficient ratio = $\gamma_a\gamma_b/\gamma_c$

Application of the mass conservation law

We consider only dissolved species in the diffusion layer, mackinawite being precipitated on the casing wall

$$Fe_{tot} = Fe^{2+}_{(free)} + FeHCO_3^+ + FeCO_3 + FeCl^+ + Fe(HS)_3^- + Fe(HS)_2 \quad (18)$$

$$CO_{3tot} = H_2CO_3 + HCO_3^- + CO_3^{2-} + FeHCO_3^+ + FeCO_3 + NaHCO_3 + NaCO_3^- \quad (19)$$

$$H_{tot} = H^+ - OH- + 2\,H_2 + FeHCO_3^+ + NaHCO_3 + 2\,H_2CO_3 + HCO_3^- + 1.H_2S \quad (20)$$

$$HS_{tot} = HS- + H_2S + 2\,Fe(HS)_2 + 3.Fe(HS)_3^- \quad (21)$$

Remarks: under the pH (6.2-6.5) and temperature (45-85°C) conditions existing in the Dogger aquifer, H_2S is in equilibrium with HS- (this was confirmed by SOLMINEQ and TPDEGAZ). We have ignored the second dissociation of H_2S and assume that HS- is a simple species. The OH- term is special: it was considered to be like a simple species and therefore does not produce H^+ by second dissociation, it was taken to be negative because it consumes H^+ ions.

Transport equations-application of Ficks law

Example of application of Fick's law to the iron

$$J_{Fe,tot} = -D_{Fe}\,\partial Fe_{tot}/\partial x \quad (3')$$

$$\text{Or } Fe_{tot} = Fe^{2+}_{(free)} + FeHCO_3^+ + FeCO_3 + FeCl^+ + Fe(HS)_3^- + Fe(HS)_2 \quad (22)$$

after the replacement of total iron by its different components, the expression is derived twice relative to the variable x (dx represents the thickness of the diffusion layer).

The application of Fick's law to the four species cited in the expression of the law of conservation of mass gives a system of non-linear differential equations. To these four equations must be added that of the electrical neutrality of the solution and that of the precipitation of mackinawite (expression of the solubility product).

The resolution of this system of equations makes it possible to draw up a profile of concentrations in the diffusion layer. This system will also be used subsequently for modelling corrosion in the walls of steel tubing. Experiments are currently in progress (using measurement of impedance and polarization resistance techniques) to study the behaviour of the carbon steel API K55 in an actual geothermal medium (Amalhay ***et al.,*** 1995).

2.6. Proposed model

It has been shown above that the diffusion layer was of the order of ten microns thick, but this was the case of a bare metal, without any scale on its surface. Therefore, for a metal covered with scale, the thickness of the scale must be added to that of the diffusion layer. Knowing that the scale can reach several millimetres, even as much as centimetres in thickness, the initial thickness of the diffusion layer becomes negligible, and its true thickness will be that of the scale. It is for this reason that relatively high thickness values are used in the calculations that follow, in order to be able to appreciate the effect of the thickness of this layer on the results obtained. We shall therefore present here an initial, simplified method for simulating the formation of scale on casing walls. Although this first method does not use Fick's law of diffusion, it nevertheless makes it possible to have an idea of the results that can be expected when this law is applied. It also has the advantage of taking into account all the simple and compound species and especially the free gases (because of the degassing of the geothermal fluid at low pressure) figuring in the code laid out below.

We began by using the TPDEGAZ code, developed by Czemichowski-Lauriol (1988) which models the evolution of geothermal fluids according to variations in their temperature (T) and pressure (P). Thus for each P-T couple, the distribution of dissolved species and the saturation indexes of the various minerals that may precipitate are calculated, and if degassing occurs, the bubble point pressure and the composition of the gaseous phase are also calculated. By calculating the saturation indexes with respect to the various minerals, the code enables an assessment of the risk of scaling in the well, but does not evaluate the amount of solid that

will precipitate Using this code, a simplified simulation of scaling phenomena as a function of time and of depth in the casing was done This assumes

(i) Uniform input of iron into the solution limited to the diffusion layer (fig 2), which takes place according to the reaction

$$Fe \rightarrow Fe^{2+} + 2e' \quad (1)$$

and the other half reaction of reduction of H^+ ions as

$$2H^+ + 2e^- \rightarrow H_{2\,(d)} \quad (2)$$

followed by $H_{2\,(d)} \rightarrow H_{2\,(g)}$ (23)

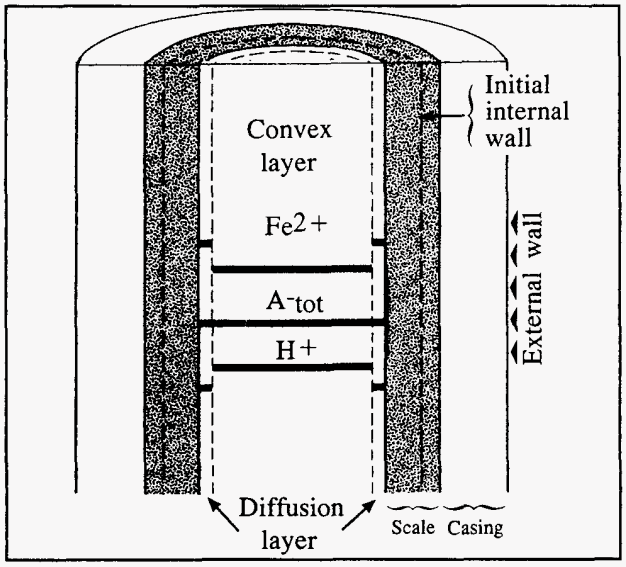

Figure 2: Concentration profiles of Fe^{2+}, $H^+$and **A-** in the proposed model.

(ii) Uniform total concentration of the other species in the diffusion and convex layers (i e no concentration gradient)

(iii) Precipitation and deposition of mackinawite Fe_9S_8, the most abundant iron sulphide in the scale, on the casing walls The elimination of precipitated FeS from the fluid and the production of H^+ occur according to the following reaction

$$Fe^{2+} + HS^- \rightarrow FeS_{(s)} + H^+ \quad (24)$$

The condition (14) has been respected to evaluate the quantity of mackinawite precipitated then deposited on the casing walls, with however, the hypothesis that only the free dissolved iron participates in this equilibrium. In the future, the two possible cases will be considered: [Fe] = dissolved free iron content or total dissolved iron content. This should increase the quantity of precipitate because the simulations with computer codes indicate that some iron complexes are present at concentrations much higher than that of free iron.

(iv) Calculation of the new diameter of the casing, by taking into account the thickness of iron dissolved and of scale deposited.

(v) Calculation of the new distribution of dissolved species after elimination of the iron that will have precipitated.

The following sequences were added to TPDEGAZ to obtain the MODEP code:

(i) The iron input from corrosion is assumed to be localised in the diffusion layer.

(ii) The test of the Ionic Activity Product (IAP) of mackinawite: if the saturation index of solution with respect to mackinawite ($\Omega_{mack} = IAP/K_{s\,mack}$) **is** less than one, the model calculates the new diameter by taking into consideration the dissolved iron. If Ω_{mack} is greater than one, it will calculate the excess of iron, eliminate it from solution, calculate the new distribution of dissolved species and the new diameter of the casing by also taking into account the iron sulphide precipitated and deposited on the casing wall.

(iii) Calculation of reaction time: the MODEP code simulates the rise of n segments in steps of ΔZ, each of which corresponds to a head loss of ***AP*** (n being chosen by the user), with the ith segment will passing through a casing with a modified diameter calculated in the following manner:

$$d_i = d_{i-1} + 2.(\text{thickness of iron dissolved})_{i-1} - 2.(\text{thickness of scale})_{i-1} \quad (25)$$

3. RESULTS AND DISCUSSION

3.1. Simulation of pH, Ω_{mack} and evolution of casing diameter

The test site is a geothermal project in the North of Paris using an submerged pump and subjected to a uniform corrosion of 600 µm/year in the casing and in the riser pipe. The geothermal fluid has a high sulphide content, **33** mg/l (10^{-3} M). The effect of the thickness e of the diffusion layer (DL), on the pH and the saturation index of the fluid with respect to mackinawite was studied for the four following cases: no DL; e = 1, 0.1 and 0.01 cm. The iron concentration increases as the thickness decreases, and thus saturation with respect to mackinawite is reached for progressively deeper zones. The increase in iron concentration in the diffusion layer causes a decrease in the concentration of H^+ ions, i.e. an increase in pH. The new equilibria bring about a change of pH. Figure 3 enables comparison of the pH calculated by MODEP with that calculated by TPDEGAZ in the absence of a diffusion layer. **A** similar pH is obtained at each step, validating the calculation done by MODEP. It is logical that the pH calculated by MODEP will be slightly higher, because at each increment two H^+ ions are consumed by reaction (2) while only one is produced by reaction (24).

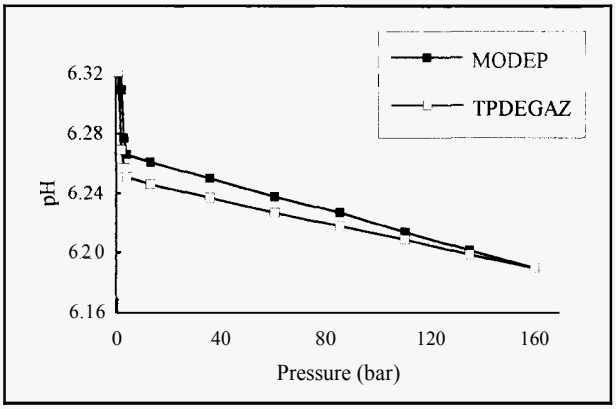

Figure 3 Comparison of pH calculated by MODEP and TPDEGAZ

Note: The addition of the mackinawite precipitation reaction brings into question the validity of using thermodynamics alone for simulating precipitation processes. This simplifying assumption **is** justified by the predominance of mackinawite in the scale encountered (because of its relatively rapid precipitation kinetics), and the lack of kinetic data concerning these reactions. Experiments are in progress to improve knowledge in this domain (Peyrot *et al.,* 1994)

Figure 4 shows the variation of pH as a function of fluid pressure and the thickness, e, of the diffusion layer. For a given pressure, the variation in pH becomes exponential as e decreases. The layer corresponding to e = 0.01 cm shows that the pH may reach very high values in the diffusion layer, thus promoting precipitation and the deposition of iron sulphides.

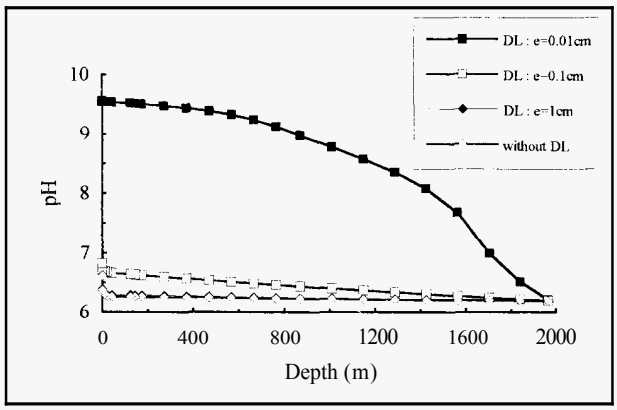

Figure 4: pH versus well depth for different thicknesses of the diffusion layer.

Figure 5 represents log Ω_{mack} as a function of the depth of the well for the four cases previously cited. A quasi-stationary regime is reached in each case owing to the precipitation of the excess iron. The increase in Ω_{mack} at the end of its passage is caused by the degassing of the fluid.

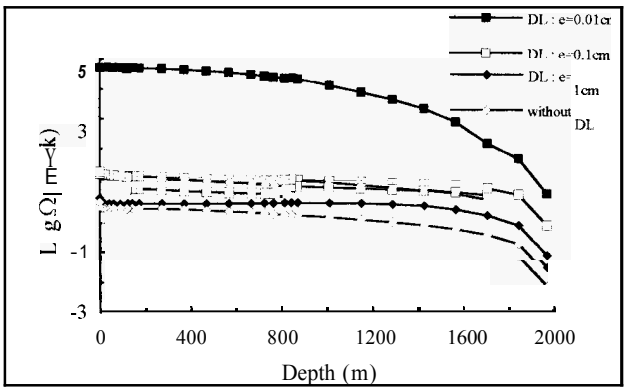

Figure 5: Log Ω_{mack} versus well depth for different thicknesses of the diffusion layer.

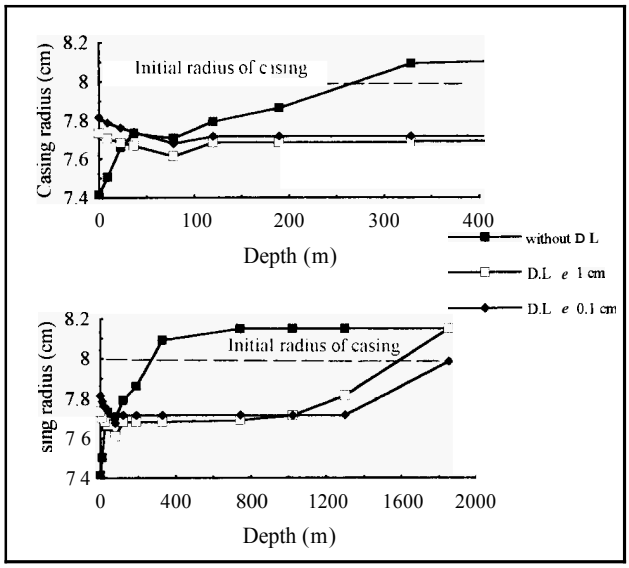

Figure 6: Casing radius versus well depth after 2.9 years of exploitation time. The different curves correspond to three diffusion layer thicknesses.

Figure 6 shows the variation in casing radius versus well depth after 2.9 years of exploitation (in the absence of a diffusion layer and with two given thicknesses of diffusion layer, e = 0.1 and 1 cm, but with no corrosion in the riser pipe above the pump). As can be expected from figure 5, scale is encountered at greater depth when e decreases but the difference between diameters decreases after the beginning of scaling where there is no diffusion layer. In the entrance of the riser pipe (120 m), the geothermal water is more saturated in iron in the two cases with a diffusion layer, and excess iron then precipitates and is eliminated more quickly (than with no diffusion layer) at the bottom of this riser pipe This decreases deposition at the wellhead.

3.2. Test of the MODEP code

Within the framework of this study, results from chemical analyses of two fluids obtained with special sampling techniques were investigated.

Sampling of fluid at the well bottom with a special composite

sampling was done at the Orly 1 production well, an artesian well. A Well Bottom Treatment Tube (WBTT) running from the shoe to the surface and made entirely of composite was specially installed. With this setup, the samples are never in contact with a metal surface and

Samples obtained	$[Fe^{2+}]$ (mg/l)	$[S^{2-}]$ (mg/l)
at the head of the WBTT (measured values)	0.73	2.84
at the production wellhead (measured values)	3.20	2.13
at the production wellhead (calculated with MODEP)	2.75	1.88

10^{-5}

Samples obtained	$[Fe^{2+}]$ (mg/l)	$[S^{2-}]$ (mg/l)
at the PRINPIMO bottom sampler (measured values)	0.60	0.57
at the production wellhead (measured values)	1.55	0.57
at the production wellhead (calculated with MODEP)	1.53	0 56

Boisdet A., Bray P., Ignatiadis I. and Abou Akar A. (1992) - *Study of corrosion and scaling in low enthalpy geothermal systems.* Rapport final IMRG du contrat CCE Joug-0005-C, rapport BRGM R36103 IRG/SGN 92, 312pp.

Crolet J.L. (1988) - Mecanismes de la corrosion uniforme sous dépôt de corrosion, *Mét. Corr. Ind.*, *63,* n° 757, pp. 279-302.

Crolet J.L. (1990) - Electrochimie de la corrosion sous dépôt dc corrosion. *Mét. Corr. Ind.*, 64, n° 764, pp. 91-106.

Czernichowski-Lauriol I. (1988) - *Modélisation de l'évolution des fluides géothermaux lors de leur exploitation pur forage.* These Universite de Nancy, 196pp.

De Waard C. and Milliams D E. (1975) - Carbonic acid corrosion of steel *Corrosion*, 31 n°5, pp. 177-181

Grande W.C. and Talbot J.B. (1993) - Electrodeposition of thin films of nickel-iron. II Modeling *J. Electrochem. Soc.,* Voi. 140, n° 3, pp. 675-681

Ignatiadis I. and Peyrot N. (1995) - Estimation of the solubility product of the iron sulphide controlling Fe^{2+} and S^{2-} solubilities in geothermal waters. *(Submitted to "European Union of Geosciences 8", Strasbourg, 9-13 April 1995).*

Kharaka Y.K., Gunter W D , Aggarwal P.K., Perkins E.H and Debraal J D. (1988) - *SOLMINEQ.88: A computer program for geochemical modeling of water-rock interactions.* U.S. Geological Survey, Water-Resources investigations Report 88-4227 Menlo Park, California, 420pp.

Nesic S. (1993) - *Prediction of transport processes IN CO_2 corrosion.* Institutt for energiteknikk. Norway. internal report, pp. 539-550.

Peyrot N. (1993) - *Contribution à l'étude de la cinétique de formation des sulfures de fer en solutions géothermales reconstituées.* Rapport de stage de DEA de Cinetique Chimique Appliquée, Université d'Orléans-BRGM, 28 juin 1993, 48pp.

Peyrot N., Ignatiadis I., Amalhay M. and Abou Akar A (1995) - Experimental concentration versus time curves for the iron (II) sulphide precipitation reaction in partly reconstituted geothermal waters and their interpretation *(Submitted to "European Union of Geosciences 8", Strasbourg, 9-13 April 1995).*

Pillay B. and Newman J. (1993) - Modeling diffusion and migration in dilute electrochemical systems using the quasi-potential transformation. *J. Electrochem. Soc.*, Vol. 140, n° 2, pp. 414-420.

Pourbaix M. and Pourbaix A. (1981) - Diagrams of chemical and electrochemical equilibria. 22nd CEFA Seminar - *Proceedings of a NATO advanced research workshop.* Centre Belge d'Etude de la Corrosion, Technical reports, Vol. 142, August 1982.

Sharland S.M. and Tasker P W. (1988) - A mathematical model of crevice and pitting corrosion. I. The physical model. *Corrosion Science*, Vol. *28,* n° 6, pp. 603-620.

Sharland S.M. (1988) - A mathematical model of crevice and pitting corrosion. II. The mathematical solution. *Corrosion Science,* Vol. *28,* n° 6, pp. 621-630.

Walton J.C. (1988) - Mathematical modeling of large-scale nonuniform corrosion: coupling of corrosion, transport, and geochemical processes in nuclear waste isolation. *Nuclear and Chemical Waste Management*, Vol 8, pp. 143-156.

Watson M. and Postlethwaite J. (1990) - Numerical simulation of crevice corrosion of stainless steels and nickel alloys in chloride solutions. *Corrosion*, pp 522-530.

Wolery T.J., Jackson K.G., Bourcier W.L., Bruton C.J., Viani B.E., Knauss K.G. and Delany J.M. (1988) - The EQ3/6 software package for geochemical modeling· current status. *In:* Chemical modeling in aqueous systems II, D.C Melchior and R.L. Basset (Ed), American Chemical Society Symposium Series, Los Angelos, CA, 25-30 September 1988, 14pp.